Available online at www.sciencedirect.com

ScienceDirect

Procedia Engineering 175 (2017) 116 – 123

Procedia Engineering

www.elsevier.com/locate/procedia

1st International Conference on the Material Point Method, MPM 2017

A penalty function method for modelling frictional contact in MPM

Fursan Hamad[a,*], Shreyas Giridharan[a], Christian Moormann[a]

[a]*Institute of Geotechnical Engineering, University of Stuttgart, Pfaffenwaldring 35, 70569 Stuttgart, Germany*

Abstract

Frictional contact is commonly represented in the Material Point Method (MPM) by algorithms based on multi-velocity fields, in which the correction is performed at the background computational mesh. Typically for applications of various stiffness values, these algorithms show a non-physical variation in the contact stresses along the interface surface. The lack of a smoothening function in the detection procedure, which is essential in explicit finite element algorithms, contributes to the stress oscillation and causes a gap between the bodies in contact. For MPM versions with a finite particle size, like Convected Particle Domain Interpolation method (CPDI), the effect of the last shortcoming becomes more pronounced. Results can be improved by using denser mesh, however, the computational cost will increase considerably.

In the present paper, the boundary of a continuum object is discretised separately from the MPM discretisation and traced accurately during the solution advancement. Therefore, contact forces among different boundaries are evaluated using a penalty function method commonly implemented in Lagrangian analyses. These forces are then mapped to the computational mesh, where the momentum equation is solved, as an external force. The suggested approach is validated with a benchmark problem, where the closed-form solution is available, and compared to the classical MPM contact algorithm. Furthermore, an application of two bodies collision with large deformation is demonstrated.

Peer-review under responsibility of the organizing committee of the 1st International Conference on the Material Point Method

Keywords: penalty function; MPM; CPDI; frictional contact.

1. Introduction

Modelling frictional contact in mechanical engineering is a widely encountered problem, which has been effectively simulated by MPM. Some of the recent applications that involve interaction of objects and being applied for various engineering disciplines are presented in [1–5]. As the standard MPM formulation provides an automatic no-slip condition, Bardenhagen et al.[6] introduce the early contact algorithm to relax the interaction between objects, which they improved in additional work [7]. In this approach, the contact is detected when the material points of different entities contribute to the same grid node of the background computational mesh. Therefore, interaction is activated before the actual contact is taking place. Furthermore, the lack of a smoothening function in the detection procedure causes oscillations in the contact stresses. Improvements have been introduced to refine the contact criterion and to reduce the instability associated with a large difference in stiffness of the contacting materials [8,9]. To

* Corresponding author.
E-mail address: fursan.hamad@igs.uni-stuttgart.de

Peer-review under responsibility of the organizing committee of the 1st International Conference on the Material Point Method
doi:10.1016/j.proeng.2017.01.038

avoid the non-physical behaviour that correspond to the velocity field algorithm [7,10], an approach based on the combination of multi-mesh is suggested by Hu and Chen[11], which has shown its applicability for different applications [12,13].

In spite of the efforts to improve the resolution of the interaction in MPM, the interface is often smeared over a region that is governed by the size of the background mesh. For advanced MPM versions, where spatial size is assigned to the material points like CPDI or GIMP (Generalized Interpolation Material Point) method, the opening between the bodies in contact becomes more pronounced [14–16]. Therefore, a more precise definition for the contact surface is essential, which can be ensured using a Finite Element (FE) formulation. Thus, a coupling procedure of a finite element structure with a material point continuum exhibits a more accurate and stable approach than pure MPM [17,18]. In this regard, different interaction schemes to couple FE thin-structures with fluids or solids being formulated in the MPM framework [19–21]. Chen et al.[1] advance the interaction between the MPM particles and the FEM elements by formulating a particle-to-surface contact instead of the MPM grid-based method. In this approach, the contact forces are calculated according to the Lagrange multiplier method where the MPM particles penetrate the FEM element faces, which is suitable for penetration problems.

In the present paper, the penalty function method that is often implemented in explicit FE analysis is introduced for CPDI, where the contact force in the normal direction is assumed proportionally to the residual of the impenetrability constraints and the surface stiffness. Therefore, the surface of the continuum in MPM is discretised separately from the volume discretisation. By setting an amount of mass to the interface, the surface nodes are able to follow the deformation of the continuum. Upon the equation of motion, the surface nodes of individual entities might interact according to the penalty function. Frictional forces are then traced back as an external contact force acting on the boundary.

By presenting a short summary of the contact algorithms in this section, the remaining part of the paper is organised as follows. The formulation of the contact condition in the framework of penalty function method is introduced in Section 2, whereas the improved MPM algorithm including the searching scheme and the calculation of the contact forces is highlighted in Section 3. In Section 4, the proposed procedure is first validated with the classical contact method for a problem where the analytical solution is available. Moreover, the suggested method is verified for a large deformation problem, which shows that the MPM penalty contact approach is in good agreement with a numerical solution based on FEM. Finally, the paper is concluded in Section 5.

2. Penalty function method

The treatment of the contact problem with the constrained optimisation process is a demanding task as the displacement constraints are unknown in advance. Therefore, it is often converted to a series of unconstrained optimisation problems by using the Lagrange multiplier method or the penalty method. Although the penalty method provides approximate solutions, it is widely used for its simplicity to satisfy the kinematic constraints in the weak sense. In this method, if a region Γ_c where contact violation exists, the potential energy is penalised proportional to the amount of the constraint violation by using a penalty function P, which is expressed as

$$P = \frac{1}{2}\omega_n \int_{\Gamma_c} g_n^2 \, d\Gamma_c + \frac{1}{2}\omega_t \int_{\Gamma_c} g_t^2 \, d\Gamma_c, \tag{1}$$

where, ω is the penalty parameter, g is the gap function, and the subscripts n and t refer to the normal and tangential direction, respectively. By adding Equation 1 to the total potential energy, the constrained minimisation problem is converted to an unconstrained minimisation problem [22]. The contact variational form is obtained from the variation of Equation 1, which yields

$$\delta P\left(\boldsymbol{u}, \delta\boldsymbol{u}\right) = \omega_n \int_{\Gamma_c} g_n \, \delta g_n \, d\Gamma_c + \omega_t \int_{\Gamma_c} g_t \, \delta g_t \, d\Gamma_c, \tag{2}$$

in which, δ denotes the variation of a quantity, and $\boldsymbol{u}$ in the displacement vector. The gap functions are defined as

$$g_n = \left(\boldsymbol{x}_s - \boldsymbol{x}_{\bar{s}}\right) \boldsymbol{e}_n^T \qquad \text{and} \qquad g_t = \|\boldsymbol{t}^0\| \left(\xi_{\bar{s}} - \xi_{\bar{s}}^0\right), \tag{3}$$

with $\boldsymbol{x}_s$ is the position vector of the slave node $\boldsymbol{s}$, $\bar{s}$ being the projection of s on the master segment, and $\boldsymbol{e}_n$ is the unit vector in the normal direction. The superscript 0 in Equation 3 denotes the values at previous time step, $\boldsymbol{t}$ is the tangential vector, and ξ is the natural coordinate defined as

$$\xi = \frac{1}{||\boldsymbol{t}||} \left(\boldsymbol{x}_s - \boldsymbol{x}_1\right)^T \boldsymbol{e}_t \qquad \text{and} \qquad 0 \le \xi \le 1, \tag{4}$$

where $\boldsymbol{x}_1$ is the position vector of one of the master segment ends, $\boldsymbol{e}_t$ is the unit vector in the tangential direction. Taking the variation of Equation 3 and back substituting the results to Equation 2 gives

$$\delta P\left(\boldsymbol{u}, \delta\boldsymbol{u}\right) = \omega_n \int_{\Gamma_c} g_n \, \boldsymbol{e}_n^T \left(\delta\boldsymbol{u}_s - \delta\boldsymbol{u}_{\bar{s}}\right) d\Gamma_c + \omega_t \int_{\Gamma_c} g_t \, ||\boldsymbol{t}^0|| \left(\frac{||\boldsymbol{t}|| \, \boldsymbol{e}_t^T \left(\delta\boldsymbol{u}_s - \delta\boldsymbol{u}_{\bar{s}}\right) + g_n \, \boldsymbol{e}_n^T \, \delta\boldsymbol{u}_{\bar{s},\xi}}{||\boldsymbol{t}||^2 - g_n \, \boldsymbol{e}_n^T \, \boldsymbol{x}_{\bar{s},\xi\xi}} \right) d\Gamma_c, \tag{5}$$

which is discretised to the form

$$\delta P(\boldsymbol{u}, \delta\boldsymbol{u}) \approx \sum_{i=1}^{ns} \delta\hat{\boldsymbol{u}}^T \left(\omega_n \, g_n \, \boldsymbol{C}_n + \omega_t \, g_t \, \boldsymbol{C}_t\right)_i, \tag{6}$$

where $\hat{\boldsymbol{u}}$ is the nodal displacement, ns is the number of the slave nodes that penetrate into the master segments. $\boldsymbol{C}_n$ and $\boldsymbol{C}_t$ in Equation 6 read [23,24]

$$\boldsymbol{C}_n = \boldsymbol{N} - \frac{g_n}{l}\boldsymbol{Q}, \qquad \text{and} \qquad \boldsymbol{C}_t = \boldsymbol{T} + \frac{g_n}{l}\boldsymbol{P}, \tag{7}$$

with

$$\boldsymbol{u} = \begin{bmatrix} \boldsymbol{u}_s \\ \boldsymbol{u}_1 \\ \boldsymbol{u}_2 \end{bmatrix} \qquad \boldsymbol{N} = \begin{bmatrix} \boldsymbol{e}_n \\ -(1-\xi)\,\boldsymbol{e}_n \\ -\xi\,\boldsymbol{e}_n \end{bmatrix} \qquad \boldsymbol{T} = \begin{bmatrix} \boldsymbol{e}_t \\ -(1-\xi)\,\boldsymbol{e}_t \\ -\xi\,\boldsymbol{e}_t \end{bmatrix} \qquad \boldsymbol{P} = \begin{bmatrix} \boldsymbol{0} \\ -\boldsymbol{e}_n \\ \boldsymbol{e}_n \end{bmatrix} \qquad \boldsymbol{Q} = \begin{bmatrix} \boldsymbol{0} \\ -\boldsymbol{e}_t \\ \boldsymbol{e}_t \end{bmatrix}, \tag{8}$$

where $\boldsymbol{u}_1$ and $\boldsymbol{u}_2$ are the displacement of the two ends of the master element, which has the length l. The final frictional force expressed on the slave and master nodes is written as

$$\boldsymbol{f}^{intr} = \sum_{i=1}^{ns} \left(\omega_n \, g_n \, \boldsymbol{C}_n + \omega_t \, g_t \, \boldsymbol{C}_t\right), \tag{9}$$

in which $\boldsymbol{f}^{intr}$ is the assembly of the interaction forces.

3. Improved contact algorithm

In this paper, the penalty function method is reformulated in the framework of MPM or CPDI. For this purpose, an interface surface is defined along which the penalty function method is applied. The coupling of the surface mesh with the MPM discretisation as well as the evaluation of the interface forces is highlighted in this section. In the present implementation, the algorithm is applied for a two-dimensional CPDI program. However, the formulation can be extended to three-dimensional problems in a straight forward procedure.

3.1. Discretisation of the interface surface

For the considered two-dimensional problem, the interface is discretised using two-node linear segments. Thickness is assigned to the surface so that mass is allocated to the interface nodes according to the density of the continuum. In all cases shown in this paper, a value of less than 1% of the entity thickness is assumed. Moreover, normal and tangential stiffness should be specified, which can be the same as the elastic stiffness where the nodes are attached. It is worth noting that exceeding the maximum stiffness of the system would influence the stability of the explicit procedure. On the other hand, a penetration between entities might take place if the normal stiffness is reduced excessively.

For numerical convenience and following the experience with the classical master-slave contact in the FE analysis, the definition of master and slave depends on the discretisation and stiffness of the interacted objects as well as their configuration.

In the present implementation, the bookkeeping of the surface nodes is separated from the material points database. The position, velocity, mass, stiffness, and contact forces of each node are tracked during the solution. In case the possible interaction zone is known a priori, the surface mesh can be defined for the intended region only. Within the computation process, the interface nodes follow the MPM algorithm and update their location from the velocity field obtained at the computational grid. After updating the location, a detection for the overlap of the interface nodes of different entities is performed.

3.2. Detection of a contact pair

For most of the dynamic impact algorithms implemented in explicit schemes, the searching for the contact pair consumes most of the computational time. Commercial FE software frequently adopt a bucket-sorting algorithm to reduce the number of required iteration, which is also implemented for a coupling between FEM and MPM [1]. In the present work, the detection of the contact pairs is performed in three steps, which has shown to be quite efficient and accurate. The first step is to check whether the momenta of different interface discretisations contribute to the same computational node. Elements attached to this node are then tagged as a zone containing a surface node that potentially might be in contact. Hence the next iteration will be carried out for the surface nodes that are located inside the tagged elements, which is usually much smaller than the total number of surface nodes. The second step of the search algorithm is to check if the distance between a node of an entity and another node of a different entity is smaller than a minimum search size. For the explicit procedure being adopted, where the propagating wave is restricted by the grid size during a time step, the computational grid spacing is used as the minimum search size. The last step to define a node-segment pair is to satisfy the following conditions

$$g_n < 0 \quad \text{and} \quad 0 \leq \xi \leq 1, \tag{10}$$

where the first condition ensures that the slave node penetrates into the master segment, whereas the other checks that the slave node is within the space of the master element.

3.3. Calculation of the contact forces

If a pair of a slave node and a master segment is established, the resisting force to oppose the penetration is evaluated from Equation 9. After assembling the global vectors, a predictor-corrector procedure to improve the resolution of the nodal forces can be performed. However, the error in the force estimation is assumed to be small when explicit time step is considered and therefore no iteration procedure is performed in this paper. In order to couple the surface mesh with the MPM solution, the contact forces are mapped from the one-dimensional boundary mesh to the four-node computational mesh via

$$\boldsymbol{f}_i^{cont} = \sum_{j=1}^{nc} N_i^j \, \boldsymbol{f}_j^{intr}, \tag{11}$$

in which nc is the total number of the contact nodes, N_i^j is the shape function of the computational node i being evaluated at the location of the boundary node j, $\boldsymbol{f}^{cont}$ is the contact forces expressed at the computational grid. The interaction of the bodies will contribute then to the momentum equation of an entity through

$$m_i \, \boldsymbol{a}_i = \boldsymbol{f}_i^{int} + \boldsymbol{f}_i^{ext} + \boldsymbol{f}_i^{cont}, \tag{12}$$

with m_i is the lumped mass at grid node i, $\boldsymbol{a}$ is the nodal acceleration, and $\boldsymbol{f}^{int}$ and $\boldsymbol{f}^{ext}$ are the internal and external force vectors, respectively.

4. Applications

In this section, the proposed procedure is validated with a closed-form solution of a cylinder rolling on an inclined surface and is compared to the classical MPM algorithm based on multi-velocity fields [6,7]. In the other application, the collision of two elastic rings is simulated in which a finite element solution is adopted as a reference.

4.1. Cylinder rolling on inclined plane

Owing to the present two-dimensional implementation, the problem of a sphere rolling on an inclined surface presented by Bardenhagen et al.[7] is replaced here with a cylinder. As an improved MPM version, CPDI is used in the present analysis where the proposed and the classical contact algorithms are tested. In this problem, a cylinder of radius 1.6 m is rolling on a plane of 20 m long and 0.8 m thick. The inclination of the plane for two different cases are: 60° and 45° with a corresponding surface coefficient of 0.286 and 0.495. As boundary conditions, the bottom and the sides of the plane are completely fixed. The first case will be referred to as *slip* whereas the other as *no-slip* contact case. The hyperelastic material model of Neo-Hookean is adopted with the following mechanical properties for the rolling cylinder: bulk modulus 6 MPa, shear modulus 3 MPa, and a density of 1 g/cm^3. The plane follows the same elastic constitutive model, while the aforementioned properties are multiplied by a factor of ten. A gravitational acceleration of 10 m/s^2 is considered for all cases.

A plane-strain analysis is performed using a computational mesh of a four-node regular cell of 0.4 m size. Irregular CPDI discretisation is selected, see Figure 2, in which the maximum particle size is 0.2 m. An interface layer of 0.001 m is discretised using a two-node element of 0.1 m size, which gives in total 517 linear segments. The analytical solution for the position of the centre of a rigid cylinder rolling on a surface is given by

$$d_s(\tau) = \frac{5}{2}\left(\sqrt{3} - \frac{2}{7}\right)\tau^2 \quad \text{and} \quad d_n(\tau) = \frac{5\sqrt{2}}{3}\tau^2, \tag{13}$$

with d_s and d_n being the position along the plane at time τ for the *slip* and *no-slip* case, respectively.

The numerical solution is performed by evaluating the initial gravity stresses at zero inclination, which is then followed by a sudden tilt of the plane and the cylinder. For the sake of comparison, the proposed method together with the classical MPM contact algorithm [10] are illustrated in Figure 1. In both slip and no-slip cases, the proposed scheme based on penalty function exhibits better results as compared to the MPM contact approach. The slow motion of the MPM algorithm is attributed to the initial position of the two bodies where no gap is assumed. In the formulation of the classical MPM contact, however, the detection of material points interaction is initiated within the influence of one computational grid. Therefore, the resistance force is overestimated until a gap is formed as illustrated in Figure 2. Although the initial prediction of the velocity for both numerical approaches matches the analytical values, see Figure 1, the classical method shows a variation in the linear increase of the velocity. On the other hand, the approach based on the penalty function gives a straight line for the velocity variation, except for the last part of the no-slip case.

4.2. Collision of two elastic rings

In order to validate the efficiency and accuracy of the proposed contact algorithm, the problem of two elastic rings collision is reproduced. In this problem, the interface along the interaction of the deformable bodies is severely distorted. As described in [25] and the references mentioned therein, the two rings have an inner and outer diameter of 60 and 80 mm, respectively. The two are placed 4 mm apart. Each ring has a density of 1.01 g/cm^3, bulk modulus of 121.7 MPa, a shear modulus of 26.1 MPa, and follows the Neo-Hookean model adopted earlier. An initial velocity of 30 m/s is assigned to the two rings in opposite directions. Uniform regular computational mesh of 2 mm cell size is employed, whereas the particle size of the CPDI domains is 0.5 mm. The surface is discretised with 2 mm mesh size while a friction coefficient of 0.1 is assumed.

As a reference solution, the software ABAQUS is selected where the penalty algorithm is implemented in the FE framework. In this analysis, the rings are discretised with 2 mm mesh size. Furthermore, similar routine of the constitutive model in CPDI is integrated in FEM. As depicted in Figure 3, the present algorithm is able to capture

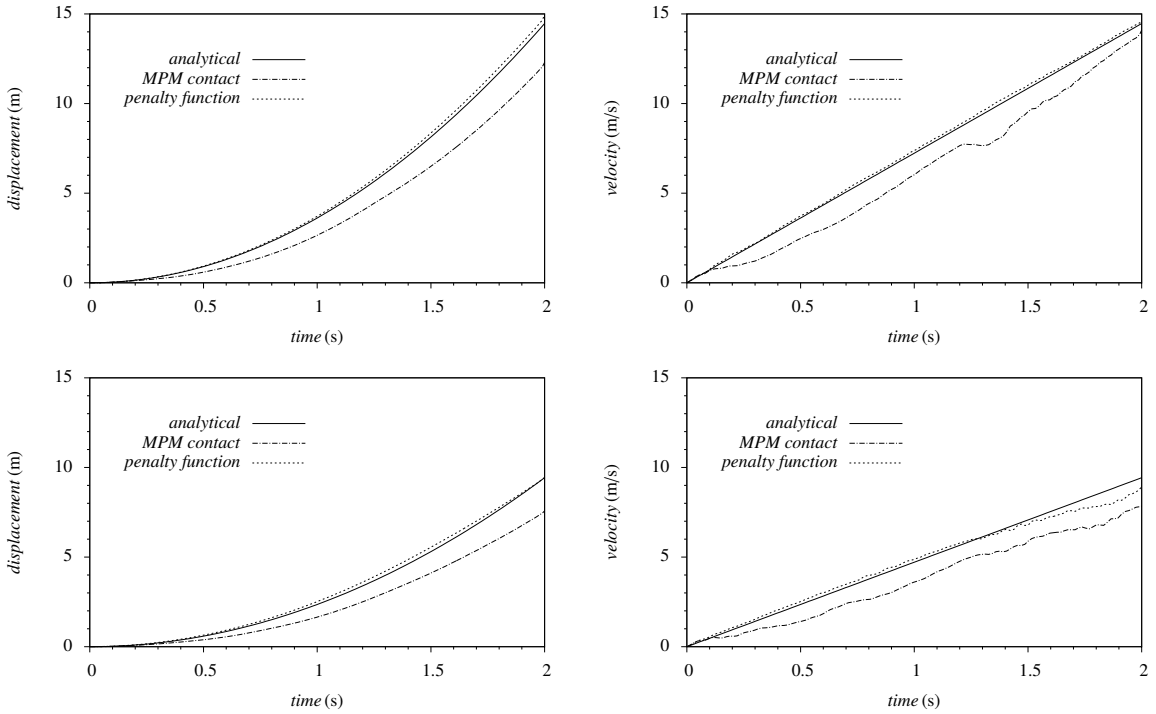

Fig. 1. Displacement and velocity of the centre point of the rolling cylinder: (upper row) slip, and (lower row) no-slip contact.

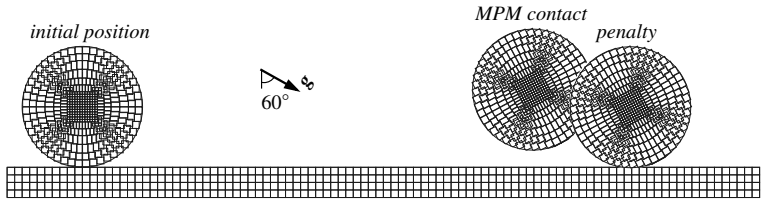

Fig. 2. Initial and finial location of the slip case of the rolling cylinder showing the gap of the MPM contact.

the highly dynamic behaviour of the collision. Moreover, the suggested mapping procedure of the contact forces to the computational grid in Equation 11 provides a weighted average of the interface forces and eventually produces fairly smooth contact stresses. For the same reason, symmetric deformations and stresses are observed across the line of symmetry. During the collision, the contact forces of the two analyses are monitored as shown in Figure 4. Although this application is considered as a multi-contact problem where the configuration of the interface is evolving during the continuous deformation, the trend shows that the contact forces of the two schemes are in good agreement. Beyond 1.6 ms, the rings are interacting at the outer edges instead of the centre point, which causes the little difference between FEM and the present CPDI analysis as shown in Figure 4.

5. Conclusions

The penalty function method that is widely used in FEM is adopted in this paper to improve the interaction in MPM. In the proposed scheme, the surface of a continuum is discretised separately from MPM so that the contact between individual entities can be performed accurately. The coupling between the background computational discretisation and the surface mesh is achieved by adding the contact forces as an external force to the momentum equation. Two

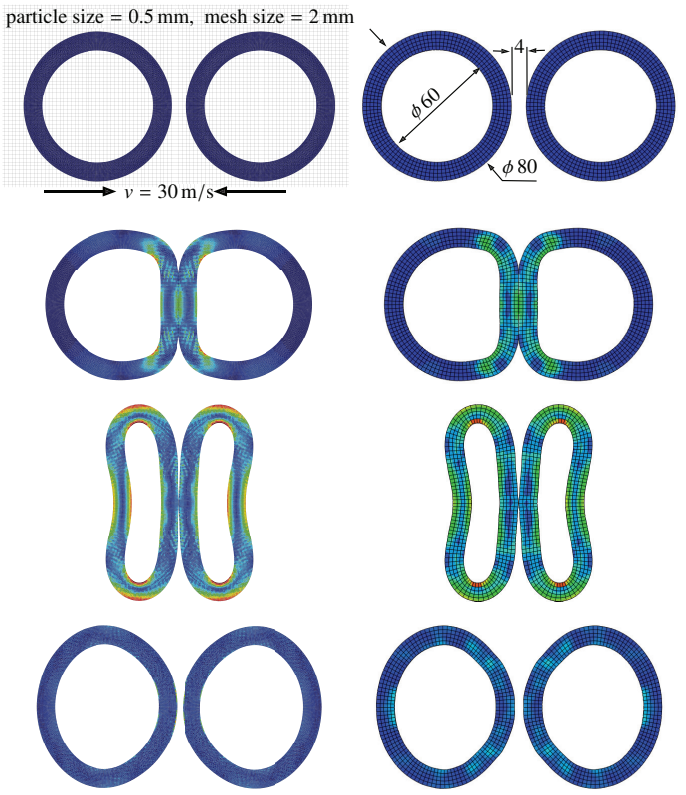

Fig. 3. Von Mises stresses (0 – 20 MPa) of the CPDI (left) and FEM (right) analyses using penalty contact algorithm at: 0, 0.4, 1.6, and 3.2 ms.

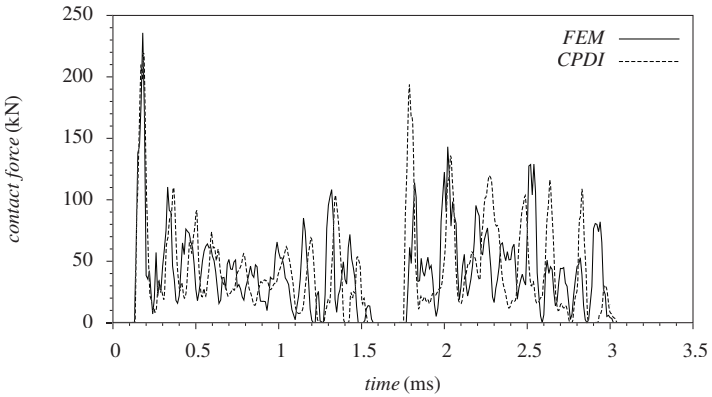

Fig. 4. Variation of the total contact forces during the collision.

numerical examples have shown that the proposed scheme is able to predict accurate and smooth contact forces.

Future work will investigate the use of a balanced master-slave algorithm instead of the classical approach being adopted as well as to study the influence of the surface mesh refinement on the resolution of the contact forces. Moreover, an algorithm to damp out the high frequency oscillations related to a highly impact problems is required.

References

[1] Z. Chen, X. Qiu, X. Zhang, Y. Lian, Improved coupling of finite element method with material point method based on a particle-to-surface contact algorithm, Computer Methods in Applied Mechanics and Engineering 293 (2015) 1–19.

[2] T. Bhandari, F. Hamad, C. Moormann, K. Sharma, B. Westrich, Numerical modelling of seismic slope failure using MPM, Computers and Geotechnics 75 (2016) 126–134.

[3] J. A. Nairn, Numerical simulation of orthogonal cutting using the material point method, Engineering Fracture Mechanics 149 (2015) 262–275.

[4] P. Liu, Y. Liu, X. Zhang, Y. Guan, Investigation on high-velocity impact of micron particles using material point method, International Journal of Impact Engineering 75 (2015) 241–254.

[5] F. Hamad, Formulation of the axisymmetric CPDI with application to pile driving in sand, Computers and Geotechnics 74 (2016) 141–150.

[6] S. Bardenhagen, J. Brackbill, D. Sulsky, The material–point method for granular materials, Computer Methods in Applied Mechanics and Engineering 187 (2000) 529–541.

[7] S. Bardenhagen, J. Guilkey, K. Roessig, J. Brackbill, W. Witzel, J. Foster, An improved contact algorithm for the material point method and application to stress propagation in granular material, CMES: Computer Modeling in Engineering & Sciences 2 (2001) 509–522.

[8] J. Ma, D. Wang, M. Randolph, A new contact algorithm in the material point method for geotechnical simulations, International Journal for Numerical and Analytical Methods in Geomechanics 38 (2014) 1197–1210.

[9] Y. Zheng, F. Gao, H. Zhang, M. Lu, Improved convected particle domain interpolation method for coupled dynamic analysis of fully saturated porous media involving large deformation, Computer Methods in Applied Mechanics and Engineering 257 (2013) 150–163.

[10] S. Bardenhagen, J. Brackbill, D. Sulsky, Shear deformation in granular material, in: 11th International Detonation Symposium, 1998.

[11] W. Hu, Z. Chen, A multi–mesh MPM for simulating the meshing process of spur gears, Computers & Structures 81 (2003) 1991–2002.

[12] P. Xiao-Fei, X. Ai-Guo, Z. Guang-Cai, Z. Ping, Z. Jian-Shi, M. Shang, Z. Xiong, Three–dimensional multi–mesh material point method for solving collision problems, Communications in Theoretical Physics 49 (2008) 1129.

[13] Z. Ma, X. Zhang, P. Huang, An object–oriented MPM framework for simulation of large deformation and contact of numerous grains, Computer Modeling in Engineering and Sciences (CMES) 55 (2010) 61–88.

[14] S. Bardenhagen, E. Kober, The generalized interpolation material point method, CMES: Computer Modeling in Engineering & Sciences 5 (2004) 477–495.

[15] A. Sadeghirad, R. Brannon, J. Burghardt, A convected particle domain interpolation technique to extend applicability of the material point method for problems involving massive deformations, International Journal for Numerical Methods in Engineering 86 (2011) 1435–1456.

[16] A. Sadeghirad, R. Brannon, J. Guilkey, Second-order convected particle domain interpolation (CPDI2) with enrichment for weak discontinuities at material interfaces, International Journal for Numerical Methods in Engineering 95 (2013) 928–952.

[17] X. Zhang, K. Sze, S. Ma, An explicit material point finite element method for hyper-velocity impact, International Journal for Numerical Methods in Engineering 66 (2006) 689–706.

[18] Y. Lian, X. Zhang, Y. Liu, An adaptive finite element material point method and its application in extreme deformation problems, Computer Methods in Applied Mechanics and Engineering 241 (2012) 275–285.

[19] F. Hamad, D. Stolle, P. Vermeer, Modelling of membranes in the material point method with applications, International Journal for Numerical and Analytical Methods in Geomechanics 39 (2014) 833–853.

[20] Y. Lian, X. Zhang, Y. Liu, Coupling of finite element method with material point method by local multi–mesh contact method, Computer Methods in Applied Mechanics and Engineering 200 (2011) 3482–3494.

[21] F. Hamad, D. Stolle, C. Moormann, Material point modelling of releasing geocontainers from a barge, Geotextiles and Geomembranes 44 (2016) 308–318.

[22] J. Arora, Introduction to optimum design, Academic Press, 2004.

[23] N. H. Kim, Y. H. Park, K. K. Choi, Optimization of a hyper-elastic structure with multibody contact using continuum-based shape design sensitivity analysis, Structural and multidisciplinary optimization 21 (2001) 196–208.

[24] J. Pfister, P. Eberhard, Frictional contact of flexible and rigid bodies, Granular Matter 4 (2002) 25–36.

[25] P. Huang, X. Zhang, S. Ma, X. Huang, Contact algorithms for the material point method in impact and penetration simulation, International Journal for Numerical Methods in Engineering 85 (2011) 498–517.